DOI: https://doi.org/10.24297/jap.v21i.9525

The effects of buckling on the electronic, thermal, and optical features of a GaP nanosheet

W. A. Abdul-Hussein

Department of Science, College of Basic Education, University of Sumer, 64005, Rifaee, IRAQ

address: w.a.abdulhussein@uos.edu.iq

Abstract

In this paper, an investigation into the electronic, thermal, and optical properties of a nanosheet made of Gallium Phosphide (GaP) via density functional theory (DFT). Our analysis focuses on the impact of buckling processes on these features. The utilization of buckling has been demonstrated to adjust the electronic thermal, and optical characteristics of a GaP nanosheet, including the energy gap, total energy, dielectric function, refractive index, and absorption coefficient. Consequently, the application of buckling in the GaP nanosheet allows for the modulation of its indirect band gap. The feasibility of synthesizing GaP nanosheets experimentally has been proven as these nanosheets exhibit both dynamic and thermal stability. Furthermore, buckling resulted in a broadening and a conspicuous shift towards lower energy in the optical phenomena as the degree of buckling increased. Therefore, it can be concluded that buckling serves as an additional parameter for enhancing the performance of GaP nanosheets in optoelectronic applications.

Keywords: Gallium phosphide, First-principles, Buckling effect, Electronic properties, Optical properties.

Introduction

Numerous objectives are pursued by nanotechnology, including sensor design, medical imaging, environmental analysis, targeted medication delivery, energy conversion, and the enhancement of electronic devices like transistors, solar cells, and diode lasers. Low-dimensional materials, mainly two-dimensional (2D) substances, are crucial in achieving these objectives [1-5].

The recent discovery of graphene has played a pivotal role in advancing the field of 2D materials. The remarkable physical features exhibited by 2D materials render them highly promising for a wide range of applications across various disciplines [6-8], this significant development has attracted a great deal of attention. Typically, the uses of pure 2D materials are limited. The lack of a discernible gap in graphene has limited its potential for utilization in nanodevices [1, 9, 10]. Consequently, various chemical and physical processes are used to modify the properties of these 2D substances, including the application of an electric field, buckling, chemical modification, and strain [11-15]. Using buckling effects to regulate the material's energy gap is a crucial stage in the growth of nanodevices. Recent research has focused extensively on how buckling influences the properties of nanostructures [16-20]. GaP, a new 2D monolayer with a narrow band gap, has been offered as an indirect semiconductor more recently. With B, Al, In, N, and Sb doping, its electronic properties, like energy band gap and density of states, in addition to the optical properties have been studied [21]. The effect of the Buckling can result from either external compressive strains or internal forces. The buckling effects can occur when the structure is under vertical compressive stress [22].

In this study, the influence of buckling on the electronic, thermal, and optical characteristics of GaP nanosheets are investigated via first-principles calculations. To accomplish this, we get the electronic and thermal properties of the GaP nanosheet under different buckling values $(0 - 1\,\text{Å})$ in increments of $0.1\,\text{Å}$ applying DFT. Time-dependent DFT (TDDFT) is then applied to some optical aspects. Results indicate that by employing the buckling effect, the ability to modify the electronic, thermal, and optical characteristics of GaP increases. Our findings provide an encouraging foundation for investigating GaP's future electronic and optical applications.

Computational method

The electronic thermal, and optical features of the GaP nanosheet were assessed through the implementation of DFT simulations using the SIESTA package [23, 24]. The exchange correlation was characterized by employing a generalized gradient approximation embodied with Perdew Burke Ernzerhof. This approach incorporates a basis set with double-ζ-polarized coupled with the utilization of Fritz-Haber-Institute pseudopotentials [25]. The utilization of the DFT-GGA, employing the single-electron estimate, is highly advantageous for the analysis of electronic structure. This approach has been subjected to extensive scrutiny regarding the impact of doping carriers on electron-electron interactions [26, 27]. The k-point grids [28] within the Brillouin zone established with the Monkhorst–Pack formulation, namely as a 12×12×1 grid. The mesh cutoff in real space is established at 150 hartrees when the system is at $300\,K$. To prevent interlayer interaction, a vacuum space with $10\,\text{Å}$ was used as the boundary condition. The structure was then optimized until the energy difference reached a value of $10^{-6}\,eV/atom$. For $1\,fs$ over $1\,ps$, Ab-initio computations of molecular dynamics (AIMD) calculations are used to examine the thermodynamic stability. The optical characteristics of a GaP nanosheet were determined using an optical broadening value of $0.1\,eV$ within the TDDFT methodology. Notably, a large number of energy bands

were considered to compute the dielectric characteristics, $\varepsilon(\omega) = \varepsilon_1(\omega) + i\varepsilon_2(\omega)$, where $\varepsilon_1(\omega)/\varepsilon_2(\omega)$ are the dielectric function real/ imaginary parts that linked together by the Kramer-Kronig relationship [29, 30]. The dielectric function is responsible for defining the optical characteristics in first-principles computations. The complex dielectric function characterizes the linear response to electromagnetic radiation. Furthermore, the absorption coefficient $(\alpha_a(\omega) = \omega\sqrt{2\sqrt{\varepsilon_1^2(\omega) + \varepsilon_2^2(\omega)} - 2\varepsilon_1(\omega)})$, the refractive index $(n(\omega) = \sqrt{\frac{\sqrt{\varepsilon_1^2(\omega)+\varepsilon_2^2(\omega)}+\varepsilon_1(\omega)}{2}})$, and the optical conductivity $(\sigma = \frac{-i\omega}{4\pi}(\varepsilon(\omega) - 1))$ are computed.

Results and discussion

We conducted DFT simulations to study the electronic, thermal, and optical properties of a GaP nanosheet characterized by a thin thickness, length of around $2.718\,nm$, and width of approximately $1.807\,nm$. Figure 1(a) illustrates the visual representation of the GaP nanosheet from top and side viewpoints. The process of GaP crystallization is characterized by the formation of hexagonal structure, which belongs to the P63/mc space group. The interatomic distance between Ga and P atoms is denoted as $d_{Ga-P} = 2.229\sim2.234$ (Å). Figure 1(c) displays the outcomes of computational analysis of the band diagram inside Brillouin zone (Figure 1(b)) and a density of states (DOS) approach to study the electronic characteristics of GaP nanosheet. Based on the computed electronic band structure, it is observed that the GaP nanosheet exhibits characteristics of a band gap-indirect semiconductor of $1.984\,eV$ at k-Γ, which exhibits a favorable level of conformity with the existing literature [21].

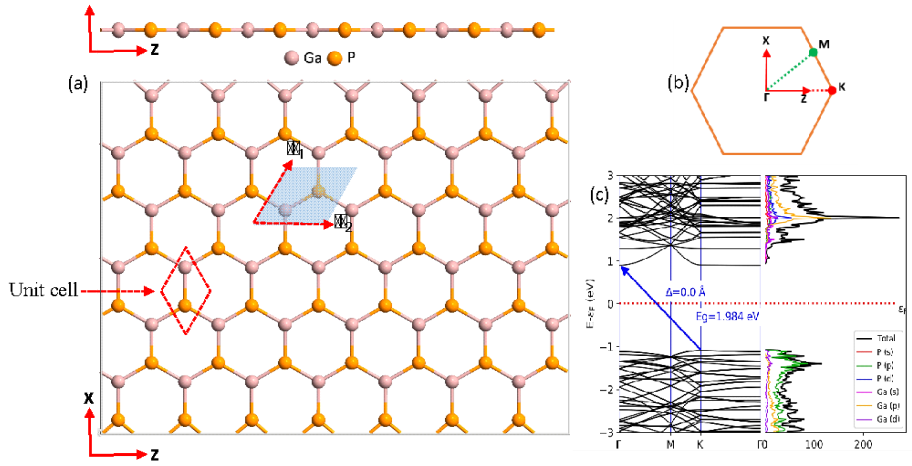

Figure 1. Top and side view (a) Brillouin zone (b) Band diagram and PDOS (c) of GaP nanosheet.

To examine the modulation of electronic characteristics in GaP nanosheets induced by the buckling effect (Δ), the buckling was applied to GaP plane with values of $\Delta = 0.0 - 1.0$ (Å). Figure 2(a–k) presents the band diagram and DOS of GaP nanosheet for various buckling values ranging from 0.0 to 1.0 Å. It is evident upon initial observation that the buckling has significantly altered the primary characteristics of the GaP band structure. Specifically, the GaP band gap experiences a steady reduction in width as the buckling value increases, as visually depicted in Figure 3.

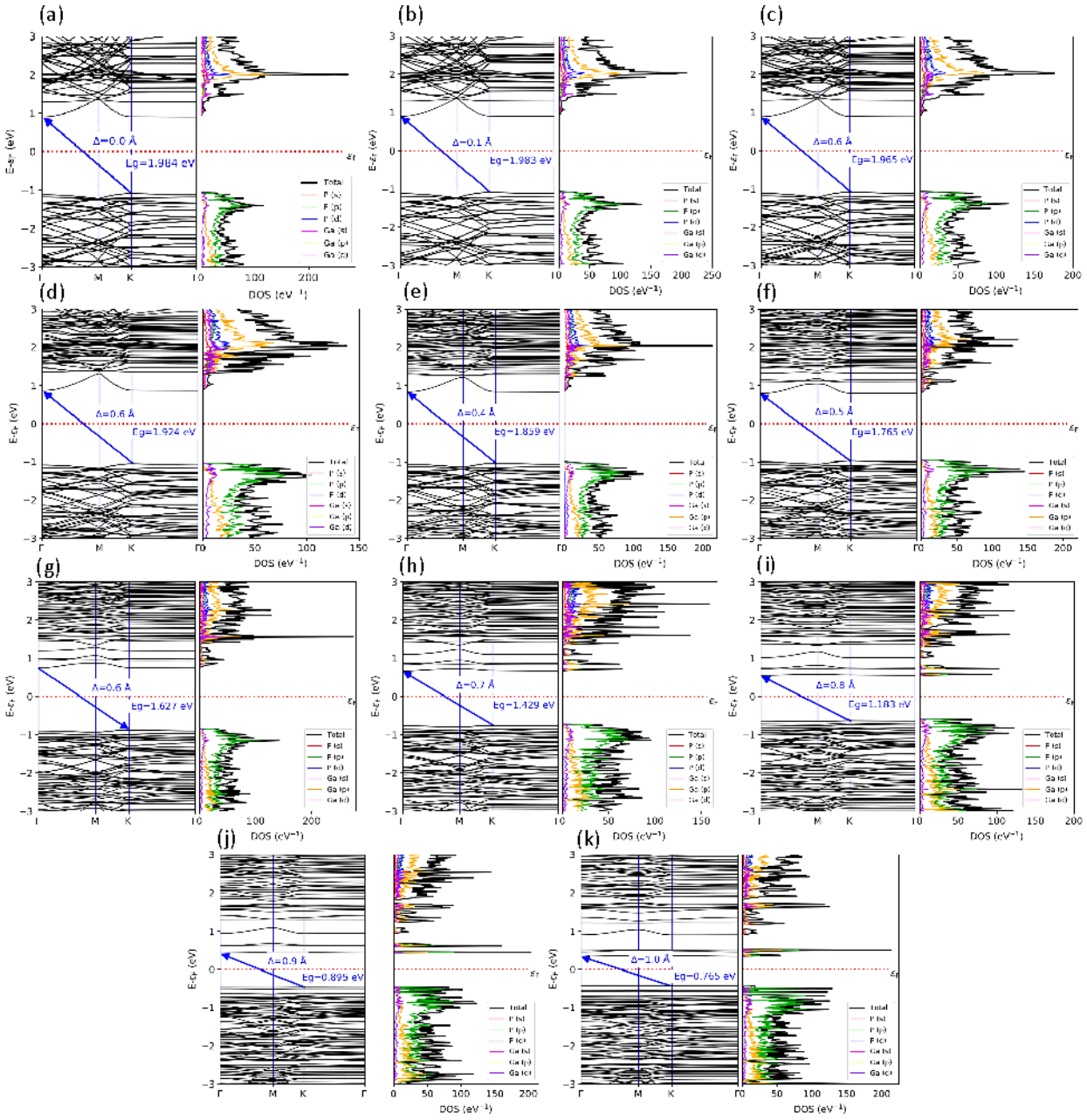

Figure 2. (a-k) Band diagram and PDOS of GaP nanosheet with different buckling values.

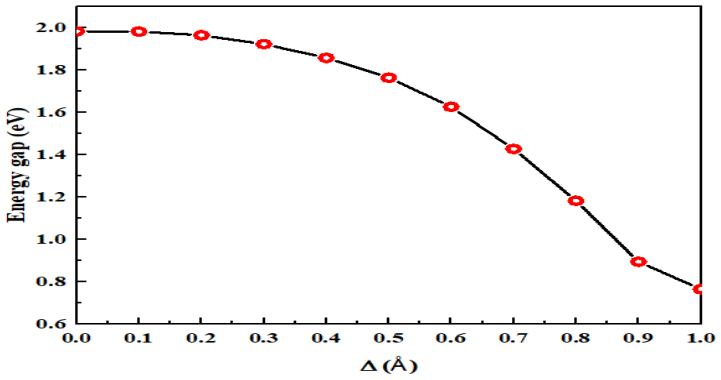

Figure 3. The band gap variation as a function of the applied buckling.

The actual applications of theoretically intended 2D materials necessitate the presence of stability as a critical factor [1]. The phonon dispersion calculation reveals the dynamic stability of the GaP nanosheet as a function of buckling, as depicted in Figure 4 (a-k), it is observed that there are no discernible imaginary modes in phonon spectrum across all wave vectors.

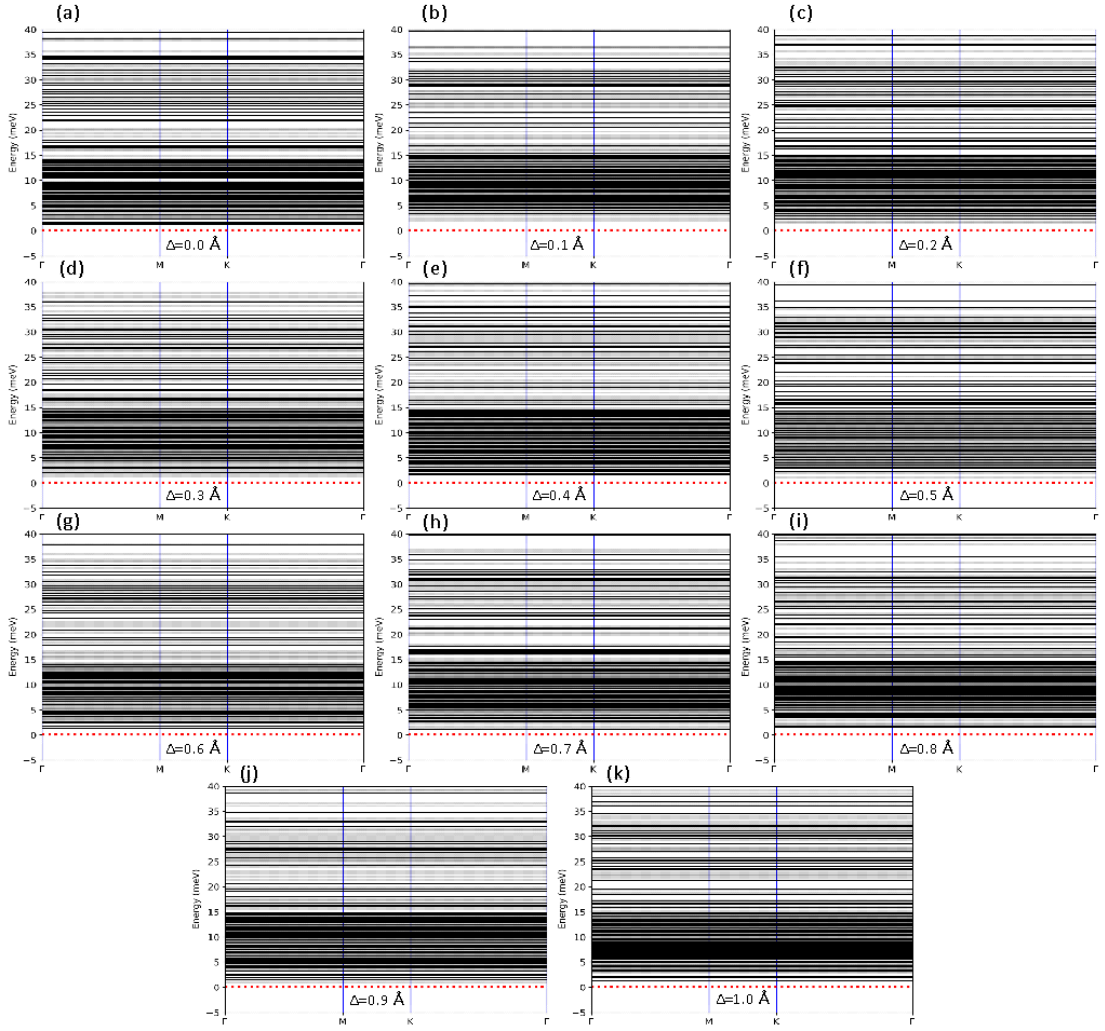

Figure 4. (a-k) Phonon spectra of GaP nanosheet as a function of buckling effects.

Additionally, we examined the impact of external temperature by the utilization of AIMD simulations under buckling values. The curves illustrate the variation of total energy with respect to the duration of molecular dynamics (MD) simulation, conducted at temperature of $1000\,K$. The stability of GaP nanosheet at elevated temperatures is seen in Figure 5. Hence, the experimental preparation of the GaP nanosheet is feasible.

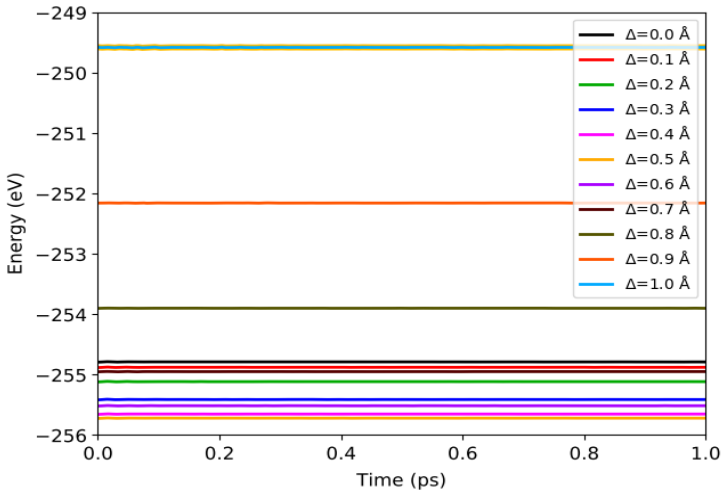

Figure 5. Total energy of GaP nanosheet under buckling effects at temperatures of $T = 1000\,K$.

The dielectric function defines the optical characteristics in first-principles computations. The complex dielectric function characterizes the linear susceptibility of semiconductor materials to electromagnetic radiation. We also calculate the index of refraction and absorption coefficient. First, we examine the $\varepsilon_1(\omega)$ and $\varepsilon_2(\omega)$ of dielectric function depicted in Figure 4. The real component of dielectric function holds significant importance as it plays a crucial role in determining both the refractive index and static dielectric constant ($\varepsilon_1(0)$) of material, where $\varepsilon_1(0)$ is the real component of dielectric function at a photon energy of zero. The value of $\varepsilon_1(0)$ for the GaP nanosheet is observed to be 1.522 that decreases to 1.423 at $\Delta = 0.4$ Å and then gradually increases to 2.476 at $\Delta = 1.0$ Å, which confirms its low dielectric nature ($k < 3.9$) and its possession of semiconductor characteristics. Also, the amplitude of $\varepsilon_1(\omega)$ exhibits dips that extend to negative values, with diminishing intensity as the buckling values increase, indicating the occurrence of plasmonic excitation [31, 32]. $\varepsilon_2(\omega)$ is an essential parameter associated with photon absorption for crystalline materials. The optical parameter exhibits an evident anisotropy when the findings for different buckling values of GaP nanosheet are compared. In the event where buckling is not present, the dominant peak in the $\varepsilon_2(\omega)$ spectrum is observed at $3.08\,eV$. The primary peak of intensity is ascribed to the transition from the P-p orbital within valence band to Ga-s orbital within conduction band, as depicted in Figure 2(a). When buckling occurs, the primary peak intensity undergoes a redshift towards lower energy, accompanied by a decrease in intensity. Additionally, a small peak in $\varepsilon_2(\omega)$ for a GaP nanosheet is appear, which increases gradually with increasing buckling. The observed phenomenon can be attributed to the redistribution of orbital hybridization and the influence of the density of states of the orbitals, resulting from the buckling effect.

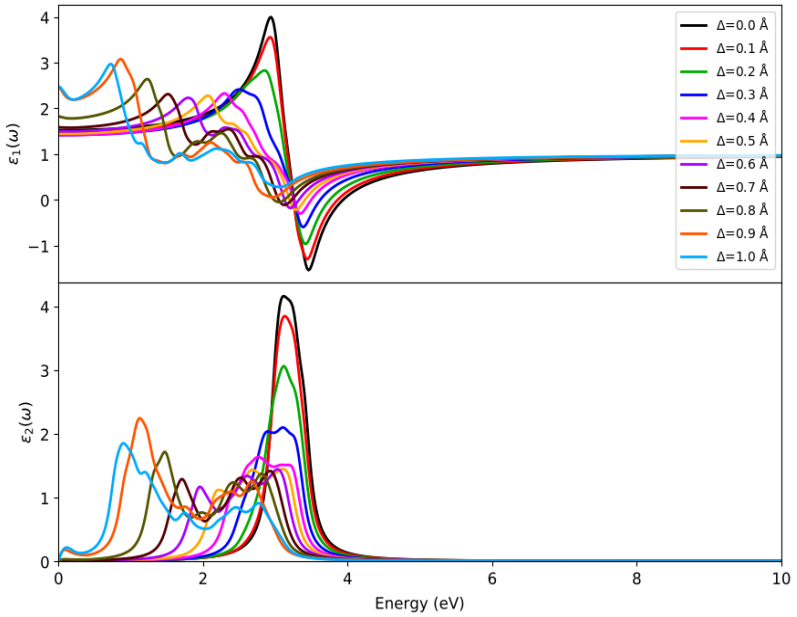

Figure 6. The real (a) and imaginary (b) components of the dielectric function as a function of the applied buckling.

The qualitative behavior of the refractive index ($n(E)$) aligns with the properties exhibited by the real section of the dielectric function, as illustrated in Figure 5. When the value of $n(E)$ is large, it indicates that there are significant interactions between the incident photons with the valence electrons, these interactions lead to a decrease in the speed of the photons as they are transmitted. The $n(E)$ value of the GaP nanosheet approaches 1.234 at the zero energy limit. However, it increases to 1.574 in the presence of buckling, namely at $\Delta = 1.0$ Å. Based on Figure 5, it can be observed that the refractive index reaches its minimum value at $3.68\ eV$. This finding suggests the presence of feeble interactions between the light photons with the valence electrons. In this instance, the majority of the incident light within the specified energy range traverses the GaP material, hence suggesting its transparency. The refractive index experiences a progressive shift to a minimum value as the buckling values increase. Eventually, it reaches a position of $3.06\ eV$ when $\Delta = 1.0$ Å, this implies that the phenomenon of transparency occurs at increased incident photon energy.

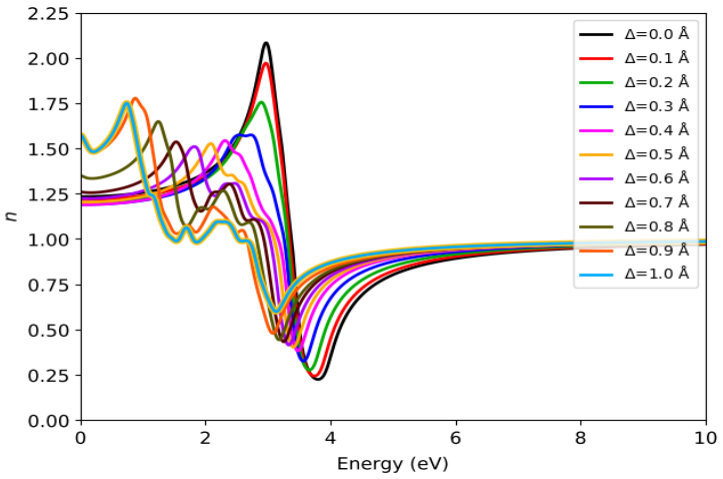

Figure 7. Variation of refractive index as a function of the applied buckling.

Figure 6 illustrates the GaP nanosheet absorption coefficient (α_a). The occurrence of a zero value for α_a suggests that the GaP nanosheet exhibits poor conduction when exposed to low-energy photons. When $\Delta = 0.0$ Å, the absorption percentage reaches its maximum value when the incident light energy is $3.38\ eV$, which decreases, broadens, and shifts at low values of photons with increasing values of buckling.

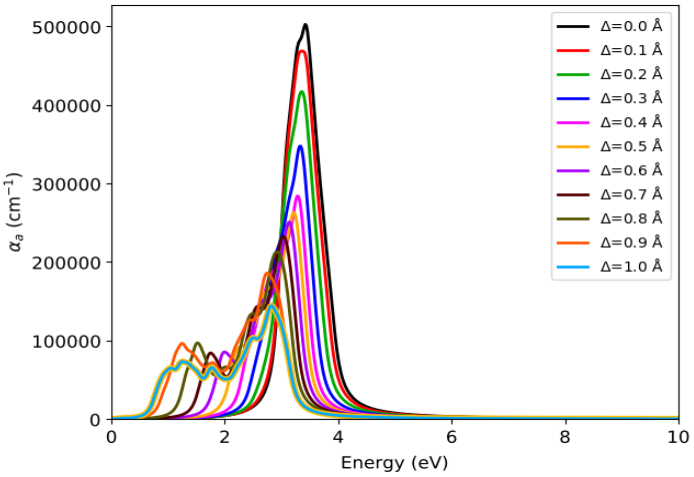

Figure 8. Dependences of absorption coefficient on the applied buckling.

Conclusions

In brief, the properties of a GaP nanosheet have been investigated using DFT, with particular attention given to the influence of buckling phenomena. The results about the electronic properties suggest that the introduction of buckling leads to an adjustable band gap, with the energy band gap diminishing as the degree of buckling increases. The observed phenomenon can be attributed to orbital hybridization redistributions and the contributions of s and p orbitals. Furthermore, the findings indicate that GaP nanosheets have both dynamic stability and thermal stability. Moreover, the experimental synthesis of GaP nanosheets has been demonstrated as feasible. The results about the optical properties indicate that the entirety of the optical spectra's characteristics experience broadening and a shift towards lower energy as the degree of buckling increases.

References

[1] W. Abdul-Hussein, F.H. Hanoon, L.F. Al-Badry, Micro and Nanostructures, 176 (2023) 207524. DOI: 10.1016/j.micrna.2023.207524

[2] A. kassaye Sibhatu, T. Teshome, O. Akin-Ojo, A. Yimam, G.A. Asres, RSC advances, 12 (2022) 30838-30845. DOI: 10.1039/D2RA05310A

[3] A. Tariq, S. Nazir, A.W. Arshad, F. Nawaz, K. Ayub, J. Iqbal, RSC advances, 9 (2019) 24325-24332. DOI: 10.1039/C9RA02778E

[4] L. Tang, X. Meng, D. Deng, X. Bao, Advanced Materials, 31 (2019) 1901996. DOI: 10.1002/adma.201901996

[5] G. Bai, S. Yuan, Y. Zhao, Z. Yang, S.Y. Choi, Y. Chai, S.F. Yu, S.P. Lau, J. Hao, Advanced Materials, 28 (2016) 7472-7477. DOI: 10.1002/adma.201601833

[6] S. Zhang, Z. Yan, Y. Li, Z. Chen, H. Zeng, Angewandte Chemie International Edition, 54 (2015) 3112-3115. DOI: 10.1002/anie.201411246

[7] A.C. Neto, F. Guinea, N.M. Peres, K.S. Novoselov, A.K. Geim, Reviews of modern physics, 81 (2009) 109. DOI: 10.1103/RevModPhys.81.109

[8] K.S. Novoselov, A.K. Geim, S.V. Morozov, D.-e. Jiang, Y. Zhang, S.V. Dubonos, I.V. Grigorieva, A.A. Firsov, science, 306 (2004) 666-669. DOI: 10.1126/science.1102896

[9] W. Zhou, S. Zhang, S. Guo, Y. Wang, J. Lu, X. Ming, Z. Li, H. Qu, H. Zeng, Physical Review Applied, 13 (2020) 044066. DOI: 10.1103/PhysRevApplied.13.044066

[10] T. Tan, X. Jiang, C. Wang, B. Yao, H. Zhang, Advanced Science, 7 (2020) 2000058. DOI: 10.1002/advs.202000058

[11] Y. Hu, C. Mao, Z. Yan, T. Shu, H. Ni, L. Xue, Y. Wu, RSC advances, 8 (2018) 29862-29870. DOI: 10.1039/C8RA05086D

[12] C. Xia, J. Du, W. Xiong, Y. Jia, Z. Wei, J. Li, Journal of Materials Chemistry A, 5 (2017) 13400-13410. DOI: 10.1039/C7TA02109G

[13] W. Yu, C.-Y. Niu, Z. Zhu, X. Wang, W.-B. Zhang, Journal of Materials Chemistry C, 4 (2016) 6581-6587. DOI: 10.1039/C6TC01505K

[14] Y. Hu, S. Zhang, S. Sun, M. Xie, B. Cai, H. Zeng, Applied Physics Letters, 107 (2015). DOI: 10.1063/1.4931459

[15] S.-M. Choi, S.-H. Jhi, Y.-W. Son, Physical Review B, 81 (2010) 081407. DOI: 10.1103/PhysRevB.81.081407

[16] W. Sheng, J.-P. Leburton, Enhanced Intraband Transitions with Strong Electric Field Asymmetry in Stacked InAs/GaAs Self-Assembled Quantum Dots, in: Physical Models for Quantum Dots, Jenny Stanford Publishing, 2021, pp. 709-719.

[17] A. Bafekry, C. Stampfl, M. Naseri, M.M. Fadlallah, M. Faraji, M. Ghergherehchi, D. Gogova, S. Feghhi, Journal of Applied Physics, 129 (2021). DOI: 10.1063/5.0044976

[18] C. Bardak, A. Atac, F. Bardak, Journal of Molecular Liquids, 273 (2019) 314-325. DOI: 10.1016/j.molliq.2018.10.043

[19] Y. Oh, J. Lee, J. Park, H. Kwon, I. Jeon, S.W. Kim, G. Kim, S. Park, S.W. Hwang, 2D Materials, 5 (2018) 035005. DOI: 10.1088/2053-1583/aab855

[20] M. Karimi, M. Hosseini, Superlattices and Microstructures, 111 (2017) 96-102. DOI: 10.1016/j.spmi.2017.06.019

[21] V. Kumar, E.V. Shah, D.R. Roy, in: AIP Conference Proceedings, AIP Publishing, 2016. DOI: 10.1063/1.4948098

[22] Y.-Q. Zhao, Q.-R. Ma, B. Liu, Z.-L. Yu, J. Yang, M.-Q. Cai, Nanoscale, 10 (2018) 8677-8688. DOI: 10.1039/C8NR00997J

[23] K. Stokbro, J. Taylor, M. Brandbyge, P. Ordejon, Annals of the New York Academy of Sciences, 1006 (2003) 212-226. DOI: 10.1196/annals.1292.014

[24] J.M. Soler, E. Artacho, J.D. Gale, A. García, J. Junquera, P. Ordejón, D. Sánchez-Portal, Journal of Physics: Condensed Matter, 14 (2002) 2745. DOI: 10.1088/0953-8984/14/11/302

[25] J.P. Perdew, K. Burke, M. Ernzerhof, Physical review letters, 77 (1996) 3865. DOI: 10.1103/PhysRevLett.77.3865

[26] W. Abdul-Hussein, F.H. Hanoon, L.F. Al-Badry, Results in Optics, 11 (2023) 100423. DOI: 10.1016/j.rio.2023.100423

[27] H. Zhong, R. Quhe, Y. Wang, Z. Ni, M. Ye, Z. Song, Y. Pan, J. Yang, L. Yang, M. Lei, Scientific reports, 6 (2016) 21786. DOI: 10.1038/srep21786

[28] H.J. Monkhorst, J.D. Pack, Physical review B, 13 (1976) 5188. DOI: 10.1103/PhysRevB.13.5188

[29] Q.-J. Liu, Z.-T. Liu, L.-P. Feng, H. Tian, Solid state sciences, 12 (2010) 1748-1755. DOI: 10.1016/j.solidstatesciences.2010.07.025

[30] B. Holm, R. Ahuja, Y. Yourdshahyan, B. Johansson, B. Lundqvist, Physical Review B, 59 (1999) 12777. DOI: 10.1103/PhysRevB.59.12777

[31] M. Fadaie, N. Shahtahmassebi, M. Roknabad, Optical and Quantum Electronics, 48 (2016) 1-12. DOI: 10.1007/s11082-016-0709-5

[32] G. Grosso, G.P. Parravicini, Solid state physics, Academic press, 2013.